Preserving Line Sinuosity in Hydrographic Feature Simplification

Lawrence V. Stanislawski[1] and Barbara P. Buttenfield[2]

1. U.S. Geological Survey, Center of Excellence for Geospatial Information Science, Rolla Missouri, U.S., lstan@usgs.gov

2. University of Colorado-Boulder, Geography Department, Boulder Colorado, U.S., babs@colorado.edu

Abstract: The preservation of stream sinuosity is an important but as yet un-emphasized process in generalization of hydrographic line features, especially when the reduced-scale data are used for mapping as well as for analysis. This paper reports initial experiments that document relations between sinuosity and map scale in hydrographic line feature data undergoing generalization processing. Thirty-eight stream sections are sampled from four scales of benchmark hydrographic data (1:24,000, 1:100,000, 1:1,000,000 and 1:10,000,000) to measure sinuosity values and change in sinuosity caused by different levels of generalization and line simplification. Empirical results indicate traditional methods of generalization and line simplification compress the variation in sinuosity values, making the data less suitable for scientific investigations involving stream sinuosity than the original source data. An alternative line simplification approach that applies a relatively constant reduction of sinuosity to each feature for a prescribed scale is proposed and tested. The simplification process uses the Bend-Simplify algorithm and iteratively adjusts the tolerance for each feature until the reduction in residual sinuosity is within target limits. The proposed approach produces distributions of sinuosity values that retain much more variability than traditional generalization methods, and that more accurately reflect the distribution of sinuosity values of the original 1:24,000-scale features than the distributions from traditionally generalized data.

Keywords: Hydrographic features, generalization, sinuosity, terrain type, slope

Disclaimer: Any use of trade, firm, or product names is for descriptive purposes only and does not imply endorsement by the U.S. Government.

1. Introduction

Cartographic generalization has been challenged for decades by the demand for simplification rules that are fully automated (Tobler, 1966; Li and Openshaw, 1992), and that generate consistent results (Shea and McMaster, 1989). Muller (1991: 457) commented on the problem following several decades of generalization research efforts, stating that "The identification of rules and their implementation into a system which can simulate the work of a traditional cartographer is one of the most difficult challenges facing the GIS research agenda of the 1990s". Savino (2011) points out that while significant progress was made in the ensuing decade, full automation is not yet achieved. A recent example of the level of automation that can be achieved for cartographic generalization is described in Stoter et al. (2014), and details of cartographic generalization being applied within several National Mapping Agencies are presented by Duchêne et al. (2014) and by Stoter et al. (2016).

Challenges persist with the generalization of terrain and hydrography data that are scale sensitive; that may vary considerably across landscape type, precipitation regime, and human settlement patterns (Buttenfield et al., 2011; Stanislawski and Buttenfield, 2011), and that must integrate vertically following simplification processing (Stanislawski et al., 2013). Effective generalization produces simplified features that are legible and retain geometric characteristics for analytic purposes, such as length, connectivity, texture, and shape, including sinuosity.

Stream sinuosity is the tendency of a stream to meander across a flood plain, and it may be estimated as the ratio of channel length to valley length (Schumm, 1973). Stream sinuosity is an important characteristic that is related to terrain slope (Lima, 2007; Lazarus and Constantine, 2013), displacement of alluvial materials (Bledsoe et al., 2008), discharge (Petrovszky et al., 2014) and flow resistivity (Lazarus and Constantine, 2013); and it can play an important role in 3-D modelling of stream channel beds (Merwade and Maidment, 2004). A number of hydrology researchers have demonstrated the complexity of such numeric relations, as for example the classic work of Langbein and Leopold (1966) who quantified the emergence of channel meanders in adjusting stream depth and velocity. Williams (1986) expanded on their work, demonstrating predictable relations between meander size (i.e., sinuosity) and specific measures of channel geometry. While studying mid-channel traces of streams on 1:24,000-scale (24K) topographic maps for plateau and lowland regions in Indiana and Kentucky, Snow (1989) showed that meander sinuosity can be modeled at scales one to two orders of magnitude larger than channel width using fractal curves, and at smaller scales by simpler geometric curves; thus establishing that predictive calculations of planform sinuosity at scale are achievable when constrained by terrain slope and roughness. Willemin (2000) shows empirically that channel sinuosity plays a primary role in stream basin shape and size.

Developing rules that preserve pattern, including sinuosity, in stream networks during generalization processing will ensure the utility of the generalized data for mapping and analysis (Zhang and Guilbert, 2016), including preservation of characteristic angularity (Gökgöz et al., 2015), which has been shown to have distinct patterns in arid and humid landscapes (Seybold et al., 2017). The research problem is to identify a logical and robust rule to estimate an appropriate amount of sinuosity to remove during simplification to smaller scales. The Radical Law (Töpfer and Pillewizer, 1966) has been used in generalization to constrain reductions of hydrographic line feature length (Buttenfield et al., 2011) in addition to reducing the number of features. However, rules that guide the adequate reduction of more complex geometric characteristics when simplifying features are not specifically defined in present literature. Sinuosity should decrease at smaller scales, which raises questions. First, is the rate of decrease linear or nonlinear, and is it constant across all scale ranges? Second, can the rate of decrease be controlled by choice of simplification tolerance, and can this constraint apply across landscape type and slope categories? This paper evaluates the relationship between the sinuosity of linear hydrographic features observed at four benchmark compilation scales with the tolerance values used to simplify corresponding features to these reduced scales. A starting point for examining rates of sinuosity reduction with scale change is modeled from the measured values.

2. Methods and Data Samples

Methods in this paper apply the Bend-Simplify algorithm (Wang and Muller, 1998) to hydrographic line features to reduce the residual sinuosity of each feature by a similar proportion. Sinuosity is computed as a ratio of the length of a vector feature through all of its vertices divided by the Euclidean distance between the start and end points of the feature. Residual sinuosity is 1.0 minus the sinuosity. For instance, a feature with a sinuosity of 1.5 has a residual sinuosity of 0.5, indicating that the feature contains additional crenulations relative to a completely straight line. Data sampling and geoprocessing are completed with ArcGIS® tools and custom Python scripts.

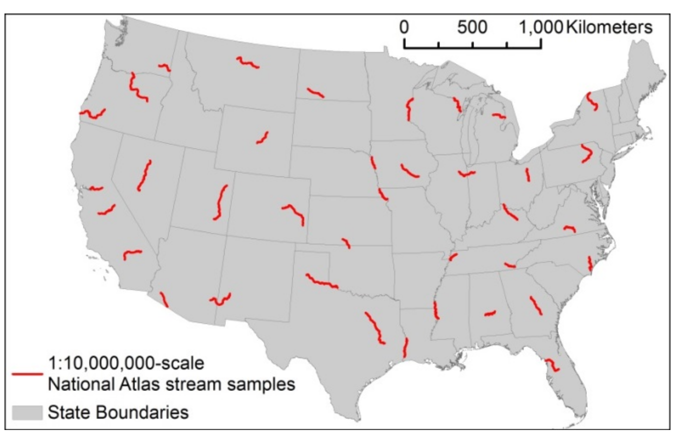

Fig. 1. Distribution of 38 linear stream features sampled from the 1:10,000,000-scale USGS National Atlas vector hydrographic dataset.

To estimate the benchmark levels of simplification implemented for linear hydrographic features at several scales, 38 sections of corresponding linear stream features were sampled from four scales of published USGS vector datasets: 24K National Hydrography Dataset (NHD), 1:100,000-scale (100K) NHD, 1:1,000,00000-scale (1M) National Atlas, and 1:10,000,000-scale (10M) National Atlas. Sample sections were initially selected from 10M National Atlas hydrographic data with the expectation that all the sampled smaller scale features are also represented in the larger scale datasets. Both headwater-to-confluence and confluence-to-confluence sections were selected from 38 rivers that are distributed over the various climate and terrain conditions in the conterminous United States (Figure 1). As defined in the 10M data, thirty-five of the samples are composed of 'river or stream' feature type, and three samples are composed of 'intermittent stream' type.

The 24K and 100K NHD were originally compiled largely from the blue-line hydrographic features on the 24K USGS Topographic maps (Stanislawski, 2009), with the 100K features being re-scribed from photo-reduced mosaics of the 24K maps. The 1M National Atlas hydrographic data are generalized from the 100K NHD using the Bend-Simplify algorithm with a 500 m tolerance (Gary et al., 2010). The 10M data were originally generalized from 1:7,500,000-scale vector hydrographic data and matched with 10M coastline features by USGS National Atlas cartographers (USGS et al., 2006).

The sample collection process first selected the larger scale features within a 5 kilometer (km) buffer around the 10M features, and then sub-selected features by the associated name from the Geographic Names Information System (GNIS) database maintained by USGS. Some subsequent editing of the selected set was necessary to ensure the features followed similar paths that start and end at nearly the same locations. Figure 2 shows the section the Alabama River (sample #33). Samples selected from the 24K NHD include over 13,000 features comprised from about 10,500 'artificial path', about 2,700 'stream/river', and 40 'connector', 'canal/ditch, or 'pipeline' feature types. 'Artificial path' features represent primary flow paths through polygonal waterbody features, such as a stream, canal, lake, or pond (USGS, 2000).

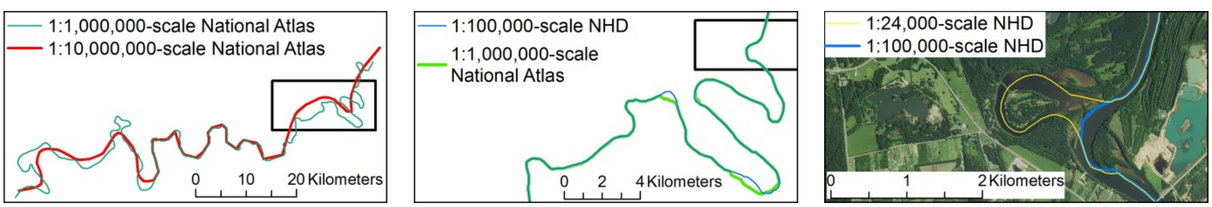

Fig. 2. Sample of vector data for a section of Alabama River selected from 1:10,000,000-scale and 1:1,000,000-scale National Atlas data, and 1:100,000-scale and 1:24,000-scale and National Hydrography Dataset (NHD) data. Black box in left panel is the boundary of center panel. Black box in center panel is the boundary of right panel, which also includes 2017 National Agricultural Imagery Program (NAIP) photography.

3. Analysis and Results

3.1 Generalized River Sections

To quantify the proportion of 24K stream sinuosity that is retained in smaller scale streams, residual sinuosity values were computed for each of the 152 samples: 38 river sections from the four scales of hydrographic data. The differences in residual sinuosity between each 24K sample and the corresponding sample from the three smaller scale datasets were computed by subtraction, and converted to a percentage of the 24K residual sinuosity. Histograms and summary statistics (mean, standard deviation, minimum, and maximum) were compiled for percent difference in residual sinuosity.

The range (maximum minus minimum) of residual sinuosity values are 1.75, 1.72, 1.37, and 0.62 for the sets of 24K, 100K, 1M, and 10M stream features, respectively. The histograms in Figure 3 show that the percent differences in residual sinuosity of the 24K sample and each of the smaller scale samples range from about -30 to 21, -48 to 13, and -96 to -9 percent for the 100K, 1M, and 10M differences, respectively. The sinuosity of most of the smaller scale samples is reduced (negative percent difference), except where a straighter and shorter human-made path exists in the 24K data. The primary issue, demonstrated by these results, is that sinuosity is altered by differing amounts in each of the generalized scales and the change in sinuosity increases and becomes less consistent with bigger scale jumps. Therefore, scientific analyses involving stream sinuosity probably are not well supported with these generalized data, particularly at smaller scales.

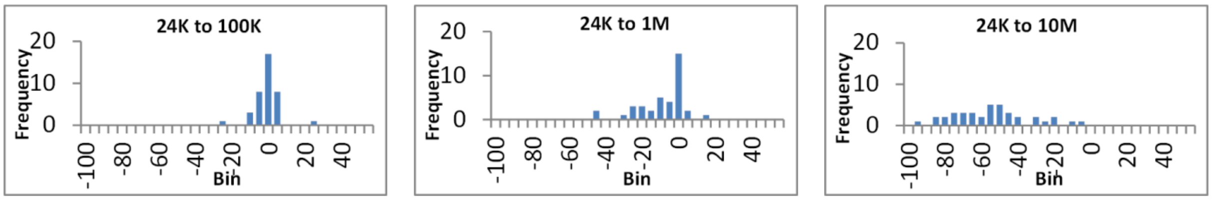

Fig. 3. Histograms of percent difference in residual sinuosity between 1:24,000-scale (24K) and three smaller scales: difference from 24K to 1:100,000-scale (100K), 24K to 1:1,000,000 (1M), and 24K to 1:10,000,000-scale (10M). Values are summarized for all corresponding samples of 38 river sections distributed over the conterminous United States.

3.2 Simplified River Sections

To assess the impact of the Bend-Simplify algorithm on hydrographic lines, the set of 24K samples were simplified with 50 meter (m), 500 m, and 5,000 m tolerance values to mimic simplification that is typical for 100K, 1M, and 10M (e.g., see Gary et al., 2010). These tolerance values are roughly equivalent to maximum positional accuracy requirements of 1/50th of an inch at the associated scales based on United States National Map Accuracy Standards (US Bureau of Budget, 1947). The tolerance for the Bend-Simplify algorithm is the minimum diameter of a circle that estimates a significant bend in a feature's shape that should be retained. All smaller bends are removed by the algorithm. After simplifying the 38 24K samples with the three tolerance values, histograms and summary statistics were compiled for percent differences in residual sinuosity between the 24K samples and corresponding features in the three simplified versions. In addition, vertices per km values were determined for each set of simplified features. The range of residual sinuosity values for the three sets of simplified features are 1.74, 1.40, and 0.65 for the 50 m, 500 m, and 5000 m tolerances, respectively. These values are very consistent with ranges of residual sinuosity values for the associated scales of benchmark data (100K, 1M, and 10M). Percent differences in residual sinuosity

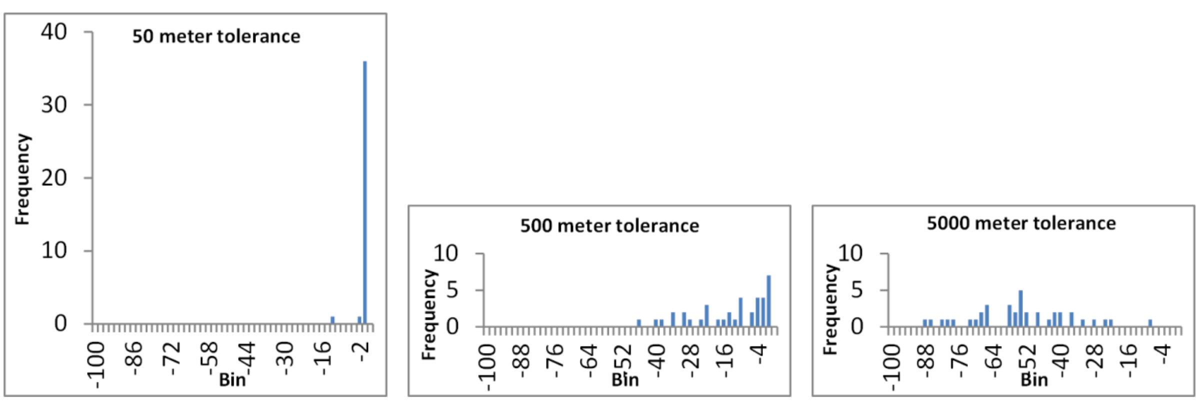

Fig. 4. Histograms of percent difference in residual sinuosity between 1:24,000 (24K) vector hydrographic line features and three levels of simplification (tolerance of 50, 500, and 5,000 meters) with the Bend-Simplify algorithm. Percent differences computed between: 24K and 50 meter, 500 meter, and 5000 meter simplifications, and summarized for all corresponding samples of 38 river sections.

of corresponding samples from 24K data to the three levels of simplification range from -13.73 to -0.0017, from -47.19 to -0.62, and from -89.16 to -8.99 for simplification with 50 m, 500 m, and 5000 m tolerances, respectively. And, median percent differences in residual sinuosity of simplified features compared with corresponding 24K features are -0.32, -10.98, and -55.21 for simplifications with 50 m, 500 m, and 5000 m tolerances, respectively. Histograms of these data are shown in Figure 4.

Comparison of Figures 3 and 4 indicate the change in sinuosity for the three sets of simplified features follows similar patterns in range and magnitude of reduction in sinuosity, with 100K similar to 50 m tolerance, 1M similar to 500 m tolerance, and 10M similar to 5000 m tolerance. However, simplification with 50 m tolerance shows less variability than the 100K data, which can be explained by the fact that 100K data were generalized through a rescribing process rather than through a single simplification operation.

3.3 Simplification Constrained to Preserve Stream Sinuosity

Empirical data presented in the previous sections demonstrate that simplification of linear streams reduces variations in stream sinuosity, which reflect climate and terrain variations. In this section, a new simplification method is tested that constrains the change in residual sinuosity for each simplified feature to a relatively constant amount in order to better preserve variability of sinuosity. Three levels of simplification effective for 100K, 1M, and 10M are generated such that the minimum reductions in residual sinuosity, as shown in Figure 4 and described in the section 3.2, are applied to all features at each scale. To meet this constraint, reductions of residual sinuosity are limited between 0.0015 to 0.0020 percent for 100K, between 0.60 to 0.65 percent for 1M, and between 8.95 to 9.00 percent for 10M, which are respective ranges centered on the minimum simplification changes produced by 50 m, 500 m, and 5000 m tolerances. The process separately simplifies each of the 38 24K sample features with the Bend-Simplify algorithm using a tolerance that meets the constraint for each target scale. Processing iteratively adjusts the tolerance for each feature until the reduction in residual sinuosity falls within the predefined limits. The constraint applied in this test case is not meant as a recommendation, but rather demonstrates a minimal level of simplification that may be achieved. Whereas larger reductions in sinuosity may be more appropriate in practice.

Table 1. Statistical summary of simplification results for 38 1:24,000-scale (24K) stream samples using the Bend-Simplify algorithm, with tolerance values adjusted to constrain the change in sinuosity to minimum levels associated with 1:100,000-scale (100K), 1:1,000,000-scale (1M), and 1:10,000,000-scale (10M) hydrographic data. Percent differences are computed as the residual sinuosity of the simplified stream sample minus the residual sinuosity of the 24K stream sample, and are expressed as a percent of the 24K residual sinuosity.

	100K Tolerance (meters)	100K to 24K Residual Sinuosity Percent Difference	1M Tolerance (meters)	1M to 24K Residual Sinuosity Percent Difference	10M Tolerance (meters)	10M to 24K Residual Sinuosity Percent Difference
Average	15.3158	-0.0026	118.1368	-0.6376	850.2632	-9.3854
Standard Deviation	14.4636	0.0016	108.6103	0.0513	935.2254	0.5947
Minimum	3.4000	-0.0085	18.0000	-0.9195	39.7000	-11.7104
Maximum	50.0000	-0.0015	445.0000	-0.6006	3915.0000	-8.9658

Table 1 summarizes statistics for tolerance values and resulting percent differences in residual sinuosity between simplified sample features and corresponding 24K features. Negative percent difference values indicate that simplification reduces the residual sinuosity of the features. Restricting the change in sinuosity to the small limits for each scale requires relatively wide ranges of simplification tolerance values from 3.4 to 50 meters, from 18 to 445 meters, and from 39.7 to 3915 meters for 100K, 1M, and 10M versions, respectively. It is not possible to find Bend-Simplify tolerance values that reduce the sinuosity of all features precisely within the target ranges. For instance, the 11.7 percent reduction of sinuosity for simplification to 10M is above the 9.00 percent target maximum. Physical limitations of the features or the granularity of the 24K representations likely control these results.

Constraining the reduction of sinuosity to the target limits results in ranges of residual sinuosity of 1.75, 1.74, and 1.60 for the 38 samples simplified to 100K, 1M, and 10M, respectively. These ranges represent 2, 27, and 157 percent higher variability in sinuosity of the simplified features compared to the benchmark features. Thus, the distributions of sinuosity values resulting from the proposed approach more accurately reflect the distribution of sinuosity values of the original 24K features than the distributions resulting from the traditionally generalized data. This method produces simplified features that are more appropriate for analytic purposes than traditionally simplified features because the correspondence to sinuosity contained in larger scale data has been preserved.

Table 2 summarizes the vertices per km before and after simplification of the 38 samples from 24K to the three smaller scales using the simplification constraints that preserve sinuosity variability. Vertices per km are also provided for the benchmark data samples for comparison. Very little change in the number of vertices per km is evident in the 100K-simplified samples, whereas the maximum number of vertices per km is reduced from about 85 at 24K to about 56 and 40 vertices per km for the 1M and 10M simplified features, respectively. The reduction in feature granularity resulting from this method of simplification is much less pronounced than traditional techniques that apply a single Bend-Simplify tolerance value to all features. In practice, larger reductions in sinuosity that also further reduce average vertices per km may be more useful from a data display and delivery perspective. For instance, it may be better to constrain residual sinuosity to the median levels of reduction that are associated with typical simplifications rather than constraining to the minimum values.

Table 2. Statistical summary of vertices per kilometer before and after simplification of 38 1:24,000-scale (24K) stream samples using the Bend-Simplify algorithm with tolerance values adjusted to constrain the change in sinuosity to minimum levels associated with 1:100,000-scale (100K), 1:1,000,000-scale (1M), and 1:10,000,000-scale (10M) hydrographic data. Values for the same stream samples from benchmark datasets are shown for comparison.

		Vertices per Kilometer					
		24K Simplified to			**Benchmark Data**		
	Source 24K	**100K**	**1M**	**10M**	**100K**	**1M**	**10M**
Average	29.770	29.405	20.687	12.005	8.721	6.083	0.375
Standard Deviation	22.854	22.768	15.411	10.589	3.536	1.565	0.105
Minimum	5.098	4.379	3.152	1.808	1.289	2.144	0.263
Maximum	84.812	84.636	56.074	40.292	14.788	10.171	0.740

Figure 5 demonstrates some of the range of geographic conditions that influence the characteristic sinuosity patterns that are evident in the sample stream lines. The Reese River is a high energy river in arid terrain with elevations ranging from 1500 to 2800 meters, having rugged slopes ranging from about 0 to 30 percent, and it is comprised of about 90 percent natural stream feature types in the 24K NHD. This river shows high frequency details evident in the small bends visible at the 100K and much less noticeable at 1:2,000,000-scale (2M). Bend-Simplify tolerances required to achieve target sinuosity values for the Reese River range from 3.7 to 40 meters, indicating that this river is highly sensitive to simplification processing. The section of the Mississippi River shows a high-volume meandering pattern in a humid, low elevation (20 to 35 m), with nearly flat slopes throughout a smooth terrain. In the 24K NHD, the linear feature type for this section of river is derived artificial flow path through a wide polygonal river. The Mississippi line features are the least sensitive to simplification, requiring Bend-Simplify tolerances from about 10 to 3900 meters to achieve the target sinuosity ranges. Figure 6 shows an example of another river in arid terrain that requires simplification tolerances between that of the Reese and Mississippi Rivers, but closer to the Reese. Elevation ranges between 900 and 2200 m for the Gila River, with slopes ranging from about 1 to 30 percent. About 50 percent of the features in the 24K NHD comprising the Gila River are artificial path through polygonal streams, with the remainder being single-line stream type. Bend-Simplify tolerances to achieve target sinuosity values for this section of the Gila River range from 3.4 to 252 m.

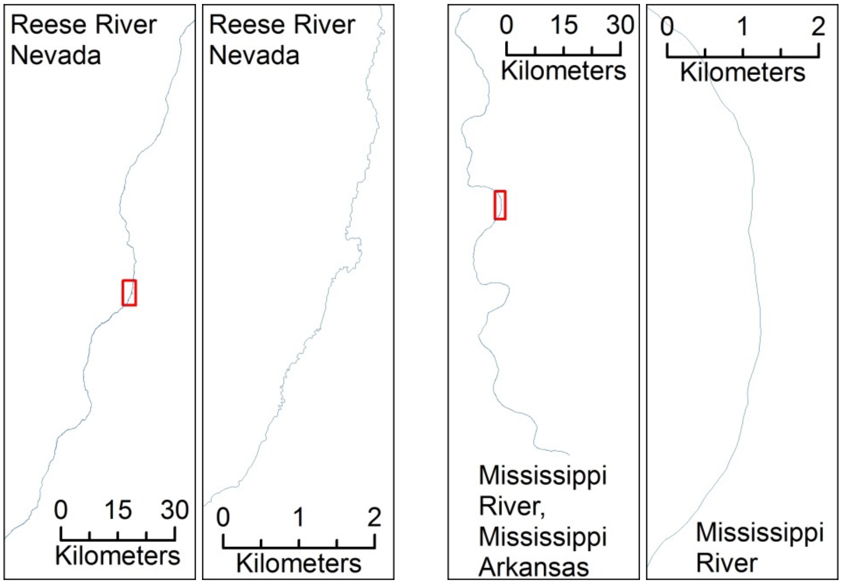

Fig. 5. Small scale (1:2,000,000) and medium scale (1:100,000) displays of sections of the Reese River in Nevada (two left panels) and the Mississippi River in Mississippi and Arkansas (two right panels). Features shown are from the 1:24,000-scale National Hydrography Dataset. Red boxes in each small scale display show the extent of the medium scale display to the right. Notice in the medium scale displays that the Reese River, from an arid region, shows a high frequency of small bends which are not evident for the Mississippi River, which is in a more humid environment.

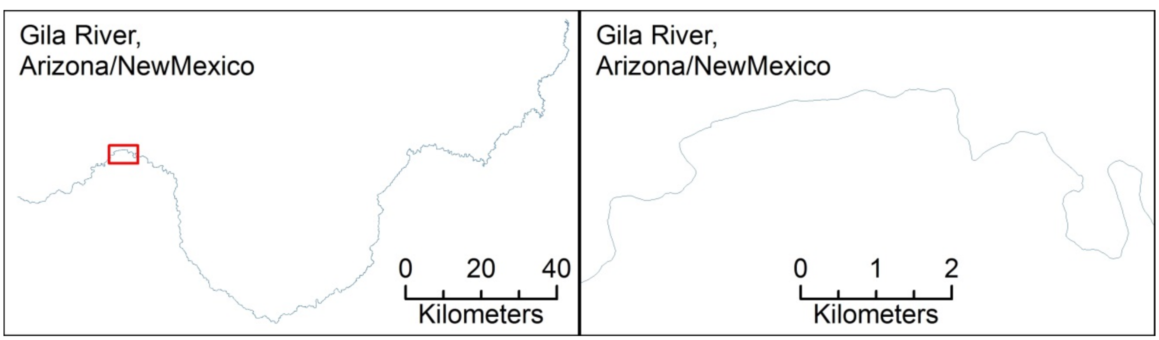

Fig. 6. Small scale (1:2,000,000) and medium scale (1:100,000) displays of section of the Gila River from an arid region in Arizona and New Mexico. Features shown are from the 1:24,000-scale National Hydrography Dataset. Red box in the small scale display at left shows the extent of the medium scale display to the right. Notice in the medium scale display that the Gila River shows intermediate frequency details which manifest as high frequency detail in the smaller scale display.

4. Summary and Discussion

Sinuosity and other stream characteristics are affected by geomorphic processes that form the features in the landscape. Topographic maps and geospatial data have enabled various synoptic evaluations involving stream channel geometry for many years, as demonstrated by measurements of river widths, channel patterns and profiles from aerial photos and topographic maps (Carlston, 1963; Brice, 1964) and analysis of river branching angles from NHD data in 2017 (Seybold et al., 2017). Consequently, preservation of sinuosity and other geometric characteristics during cartographic generalization operations has important analytic implications.

This paper reports initial experiments that document relations between sinuosity and map scale in hydrographic line feature data undergoing generalization processing. Thirty-eight stream sections are sampled from four different cartographic benchmark data sets (24K, 100K, 1M and 10M) to measure sinuosity values and change in sinuosity caused by different levels of generalization and line simplification. Empirical results indicate traditional methods of generalization and line simplification compress the variation in sinuosity values, making the data less suitable for scientific investigations involving stream sinuosity. Such reductions in detail and variability of geometric characteristics in small scale feature representations are understandable and have been expected in the past for generalized data. This research explores possible methods to simplify linear stream features in a manner that more accurately retains the geometric variability, along with positional accuracy of the data, which can better support small-scale regional or continental analyses.

An alternative line simplification approach that applies a relatively constant reduction of sinuosity to each feature for a prescribed scale is proposed and tested. The simplification process uses the Bend-Simplify algorithm and iteratively adjusts the tolerance for each feature until the reduction in residual sinuosity is within target limits. Target limits for 100K, 1M, and 10M are centered on minimum sinuosity reduction values determined from simplifications of sample 24K features with 50, 500, and 5,000 m tolerance values, respectively. The approach produces distributions of sinuosity values that retain much more variability than traditional generalization methods, and that more accurately reflect the distribution of sinuosity values of the original 24K features than the distributions from traditionally generalized data.

In the tests presented, simplification was constrained to consistently minimize reduction of sinuosity for the target scales. However, further testing is needed to find optimal constraints for sinuosity that furnish a good compromise between cartographic legibility and analytic usefulness of the resulting data. A promising alternative would apply the median level of sinuosity reduction rather than the minimum, which might retain less variability in sinuosity at the target scale, yet furnish acceptable representations for data display and delivery. Assessment of results could be improved by including displacement metrics, following arguments made by Shi and Cheung (2006) to measure displacement and shape distortion. Dual metrics can lend insights not only to shifting position of simplified line features, but also to positional uncertainty of the source data, that may propagate to the target scales during processing (Cheung and Shi 2004).

Geoprocessing of the proposed simplification algorithm was implemented through custom ArcGIS® Python scripts and was not optimized to handle large datasets, which will be necessary if the algorithm will support mapping operations. The proposed approach requires multiple simplifications of each feature. Parallel processing options that can distribute processing over multiple machines, such as in a Linux compute cluster, are being considered. It is expected that a parallel implementation of this algorithm with open source technologies on a high performance cluster will enable rapid processing of large datasets containing millions of features. However, a final workflow to fully automate this process is not yet established. A possible goal is to develop a heuristic method that adjusts to a dataset's characteristic sinuosity patterns, which as seen from this research vary uniquely across progressions of scale.

Further work on this problem can inform and advance understanding of the complex impacts of generalization processing on stream channel sinuosity. It is important to note that maintaining a constant level of reduction in line feature sinuosity for a particular scale reduces line feature lengths in similar proportion. Consequently, it should be possible to work from smaller to larger scales by essentially inverting the generalization 'transformation,' in Tobler's (1966) words, reversing the reduction in sinuosity to produce more accurate larger scale estimates of feature lengths and sinuosity. Without this examination of the progression of reduced sinuosity, simplified feature length estimates likely are less accurate and less precise. Accepting this premise assumes similar characteristics and consistent representations of sinuosity, and this warrants further examination. The rules applied in this study are designed to retain the characteristic shape of all stream features as well as the relative difference in sinuosity between features in the same scale, while reducing the density of vertices and maintaining an appropriate positional accuracy for the features. Conceivably, accurate variations in stream sinuosity values are represented in data resulting from the proposed approach in a manner that better supports scientific studies than previous alternatives.

Acknowledgements

The work of Barbara Buttenfield on this research is supported in part by the Grand Challenge Initiative "Earth Lab" funded by the University of Colorado (http://www.colorado.edu/grandchallenges/).

References

Barrault, M., Regnauld N., Duchêne C., Haire K., Baeijs C., Demazeau Y., Hardy P., Mackaness W., Ruas A., and Weibel R. (2001). Integrating multi-agent, object-oriented, and algorithmic techniques for improved automated map generalization. In *Proceedings 20th International Conference on Cartography*, ICA, Beijing, China, (3), 2110-2116.

Bledsoe, B., Hawley, R. and Stein, E.D. (2008). Stream channel classification and mapping systems: mplications for assessing susceptibility to hydromodification effects in southern California. Colorado State University, Fort Collins, CO: *Southern California Coastal Water Research Project Technical Report 562*, April 2008.

Buttenfield, B.P., Stanislawski, L.V. and Brewer, C.A. (2011). Adapting generalization tools to physiographic diversity for the USGS National Hydrography Dataset. *Cartography and GIScience* 38(3): 289-301.

Brice, J.C. (1964). Channel patterns and terraces of the Loup Rivers in Nebraska. *United States Geological Survey Professional Paper 422-D*. Washington D.C.: US Government Printing Office.

Carlston, C.W. (1963). Drainage density and streamflow: physiographic and hydraulic studies of rivers. *United States Geological Survey Professional Paper 422-C*. Washington D.C.: US Government Printing Office.

Cheung, C.K. and Shi, W. (2004). Estimation of the positional uncertainty in line simplification in GIS. *The Cartographic Journal* 41(1), 37-45. http://dx.doi.org/10.1179/000870404225019990.

Duchêne, C., Baella, B., Brewer, C., Burghardt, D., Buttenfield, B., Gaffuri, J., Käuferle, D., Lecordix, F., Maugeais, E., Nijhuis, R., Pla, M., Post, M., Regnauld, N., Stanislawski, L., Stoter, J., Tóth, K., Urbanke, S., van Altena, V., and Wiedemann, A.(2014). Generalisation in practice within national mapping agencies. In D. Burghardt, C. Duchêne, W. Mackaness (Eds.), *Abstracting geographic information in a data rich world: methodologies and applications of map generalization* (pp. 329-392). Springer International Publishing Switzerland 2014.

Gary, R.H., Wilson, Z.D., Archuleta, C.M., Thompson, F.E., and Vrabel, J. (2010). Production of a national 1:1,000,000-scale hydrography dataset for the United States: feature selection, simplification, and refinement. *U.S. Geological Survey Scientific Investigation Report 2009-5202* (revised 2010), Washington D.C.

Gökgöz, T., Sen, A., Memduhoglu, A. and Hacar, M. (2015). A new algorithm for cartographic simplification of streams and lakes using deviation angles and error bands. *ISPRS International Journal of Geo-Information* 4, 2185-2204. DOI 10.3390/ijgi4042185.

Langbein, W.B. and Leopold, L. B. (1966). River meanders: theory of minimum variance. *United States Geological Survey Professional Paper 422-H*. Washington D.C.: US Gov't. Printing Office.

Lazarus, E.D. and Constantine, J.A. (2013). Generic theory for channel sinuosity. In *Proceedings of the National Academy of Sciences* (PNAS) 110(21), 8447-8452. http://www.pnas.org/content/110/21/8447 (pdf accessed 23 Feb 2017).

Li, Z., and Openshaw, S. (1992). Algorithms for automated line generalisation based on a natural principle of objective generalisation. *International Journal of Geographical Information Systems* 6, 373–89.

Lima, A.G. (2007). Cartographic scale effect on channel slopes and stream power calculations. *Nature Precedings*, http://precedings.nature.com/documents/1359/version/1 (pdf accessed 23 Feb 2017).

Merwade, V. M. (2004). Geospatial description of river channels in three dimensions. Ph.D. dissertation, University of Texas at Austin, 237 pp. https://repositories.lib.utexas.edu/bitstream/handle/2152/1274/merwadev17585.pdf?sequence=2&isAllowed=y (pdf accessed 28 Feb 2017).

Muller, J.C. (1991). Generalization of spatial databases. In D.J. Maguire, M.F. Goodchild, and D.W. Rhind, D.W. (Eds.) *Geographical Information Systems: Principles and applications*, 2, 457-475.

Petrovszky, J., Timár, G. and Molnár, G. (2014). Is sinuosity a function of slope and bankfull discharge? A case study of the meandering rivers in the Pannonian Basin. *Hydrology and Earth Systems Sciences Discussions* 11, 12271-12290. http://www.hydrol-earth-syst-sci-discuss.net/hess-2014-406/. (pdf accessed 23 Feb 2017).

Schumm, S.A. (1973). Geomorphic thresholds and complex response of drainage systems. *Fluvial Geomorphology* 6: 69-85.

Seybold, H., Rothman, D., and Kirchner, J.W. (2017). Climate's watermark in the geometry of stream networks. *Geophysical Research Letters* 44, 2272-2280. DOI: 10.1002/2016GL072089.

Shea K.S., and McMaster, R. B. (1989), Cartographic generalization in a digital environment: when and how to generalize. *Proceedings Auto-Carto 9*, Baltimore MD: 56-67.

Shi, W. and Cheung, C.K. (2006). Performance evaluation of line simplification algorithms for vector generalization, *The Cartographic Journal* 43(1), 27-44. DOI: 10.1179/000870406X93490

Snow, R.S. (1989). Fractal sinuosity of stream channels. *Pure and Applied Geophysicis* 131(1/2): 99-109.

Stanislawski L.V., Falgout, J. and Buttenfield B.P. (2015). Automated extraction of natural drainage density patterns for the conterminous United States through high performance computing. *The Cartographic Journal* 52(2), 185-192.

Stanislawski, L.V., Buttenfield, B.P, Brewer, C.A. and Anderson-Tarver, C. (2013). Integration metrics for cartographic generalization: assessment of 1:1,000,000 scale hydrography and terrain. In *Proceedings, 26th International Cartographic Congress*, Dresden, Germany, August 2013. http://generalisation.icaci.org/images/files/workshop/workshop2013/genemappro2013_submission_15.pdf (pdf accessed 23 Feb 2017).

Stanislawski, L.V. and Buttenfield, B.P. (2011). Hydrographic generalization tailored to dry mountainous regions. *Cartography and GIScience* 38(2), 117-125.

Stanislawski, L.V., Buttenfield, B.P. and Samaranayake, V.A. (2010). Automated metric assessment of hydrographic feature generalization through bootstrapping. *Proceedings, 13th International Cartographic Association Symposium on Multiple Representations and Map Generalization*, Zurich Switzerland, September http://generalisation.icaci.org/images/files/workshop/workshop2010/genemr2010_submission_11.pdf (pdf accessed 23 Feb 2017).

Stoter, J., van Altena, V., Post, M., Burghardt, D. and Duchêne, C. (2016). Automated generalisation within NMAs in 2016. *ISPRS - International Archives of the Photogrammetry, Remote Sensing and Spatial Information Sciences XLI-B4* (June): 647–52. doi:10.5194/isprs-archives-XLI-B4-647-2016.

Stoter, J., Post, M., van Altena, V., Nijhuis, R. and Bruns, B. (2014). Fully automated generalization of a 1:50k map from 1:10k data. *Cartography and Geographic Information Science* 41 (1), 1–13. DOI:10.1080/15230406.2013.824637.

Tobler, W.R.T. (1966). Numerical Map Generalization. *Michigan Inter-University Community of Mathematical Geographers Discussion Paper #8.* Ann Arbor, MI. https://deepblue.lib.umich.edu/handle/2027.42/58252 (pdf accessed 23 Feb 2017).

Töpfer, F. and Pillewizer, W. (1966). The principles of selection: a means of cartographic generalization. *The Cartographic Journal*, 3(1), 10–16.

US Bureau of the Budget (1947). United States National Map Accuracy Standards, June 17.

U.S. Geological Survey (2000). The National Hydrography Dataset: concepts and contents (February 2000), United States Geological Survey. http://nhd.usgs.gov/chapter1/chp1_data_users_guide.pdf. (pdf accessed 27 Feb 2017).

U.S. Geological Survey, Mexican National Institute of Statistics, Geography and Informatics, Government of Canada, Natural Resources Canada, Canada Centre for Remote Sensing, The Atlas of Canada (2006). North American Atlas—Hydrography. https://pubs.usgs.gov/of/2009/1150/gis/basemap/hydro_lmeta.htm#9. (pdf accessed 28 Feb2017)

Wang, Z. and Muller, J.C. (1998). Line generalization based on analysis of shape characteristics. *Cartography and Geographic Information Science 25, 3-15.*

Willemin, J.H. (2000). Hack's Law: sinuosity, convexity, elongation. *Water Resources Research* 36(11), 3365-3374.

Williams, G.P. (1986). River Meanders and channel Size. *Journal of Hydrology* 88, 147-164.

Zhang, L. and Guilbert, E. (2016). Evaluation of river network generalization methods for preserving the drainage pattern. *ISPRS International Journal of Geo-Information* 5(12), 230. DOI: 10.3390/ijgi5120230